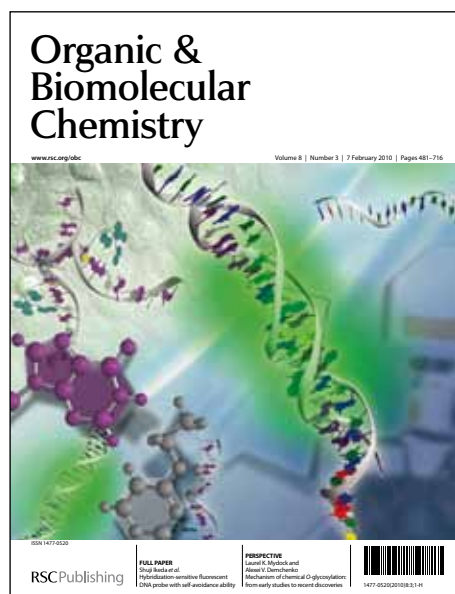


# Organic & Biomolecular Chemistry

Accepted Manuscript



This is an *Accepted Manuscript*, which has been through the RSC Publishing peer review process and has been accepted for publication.

*Accepted Manuscripts* are published online shortly after acceptance, which is prior to technical editing, formatting and proof reading. This free service from RSC Publishing allows authors to make their results available to the community, in citable form, before publication of the edited article. This *Accepted Manuscript* will be replaced by the edited and formatted *Advance Article* as soon as this is available.

To cite this manuscript please use its permanent Digital Object Identifier (DOI®), which is identical for all formats of publication.

More information about *Accepted Manuscripts* can be found in the [Information for Authors](#).

Please note that technical editing may introduce minor changes to the text and/or graphics contained in the manuscript submitted by the author(s) which may alter content, and that the standard [Terms & Conditions](#) and the [ethical guidelines](#) that apply to the journal are still applicable. In no event shall the RSC be held responsible for any errors or omissions in these *Accepted Manuscript* manuscripts or any consequences arising from the use of any information contained in them.

# Starburst dendrimers consisting of triphenylamine core and 9-phenylcarbazole-based dendrons: synthesis and property

Jia You, Guiyang Li and Zhonggang Wang\*

*State Key Laboratory of Fine Chemicals, Department of Polymer Science and Materials, School of Chemical Engineering, Dalian University of Technology, Dalian 116023, P. R. China*

---

\* To whom all correspondences should be addressed.

Email: zgwang@dlut.edu.cn

[View Online](#)

ABSTRACT: Novel dendrimers consisting of a triphenylamine core and 1st to 3rd generations of 9-phenylcarbazole-based dendrons were synthesized by Suzuki coupling reaction through convergent approach. Their structures were confirmed by two-dimensional correlated H-H COSY and C-H HSQC NMR spectra, MALDI-TOF MS and elemental analysis. The dendrimers exhibit excellent thermal stability with 5% weight loss temperatures over 540 °C. The computer modeling reveals that the dendrons in dendrimers greatly twisted with the generation, leading to the dendrimers decreased crystalline ability. Of interest is the observation that, for an identical dendrimer, the solid film displays the similar UV absorption and luminescence emission profiles to the solution sample, indicating that, after evaporation of solvent, the rigid dendrimer can well maintain its conformational morphology and the aggregation or stacking of the chromophoric groups is significantly inhibited. All the dendrimers can emit intense fluorescence with narrow full width at half maximum (FWHM) around 46-50 nm. Moreover, with the incremental generation, the quantum efficiencies remarkably increase from 64 to 95%, suggesting that the highly contorted and bulky dendrons effectively decrease energy wastage and nonradiative decay. The synergistic effect of electron-donating triphenylamine core and 9-phenylcarbazole-based dendrons results in the HOMO energy level of -5.36 eV for the 3rd-generation dendrimer, very close to the work function of the ITO/PEDOT electrode (-5.2 eV), which characteristic is very advantageous for the hole injection and transport materials.

**Keywords:** dendrimers, triphenylamine, carbazole, synthesis, optoelectronic property

## Introduction

Dendrimers are three-dimensional treelike molecules possessing well-defined structures composed of a core and various numbers of dendrons. The synthesis method of dendrimers by stepwise generation-by-generation growth ensures the batch to batch reproducibility, definite chemical structure, molecular weight and monodispersity.<sup>1</sup> These characteristics endow dendrimers with distinct physicochemical nature from linear and hyperbranched polymers in numerous aspects such as inter-molecular

aggregation, crystalline behavior, solubility and film-forming process. Dendrimers have found a wide range of applications, including drug delivery systems,<sup>2</sup> magnetic resonance imaging,<sup>3</sup> homogeneous catalysis<sup>4</sup> and optical data storage.<sup>5</sup> Recently, they have also been exploited as an active component for electronics and optoelectronics molecular devices<sup>6</sup> such as organic light-emitting diodes (OLEDs)<sup>7</sup> since the dendritic topology can effectively suppress the formation of excimers<sup>8</sup> and enhance the charge transport ability.<sup>9</sup>

The properties of a dendrimer are tightly correlated with the chemical structure of the core, dendrons and generation number. Carbazole possesses strong absorption in near-UV region, low redox potential,<sup>10</sup> intense luminescence emission,<sup>11</sup> and outstanding hole-transporting ability.<sup>12</sup> Moreover, carbazole can be easily functionalized at its 3-, 6-, and 9- position, thus conveniently covalent-linked to other molecular moieties.<sup>13</sup> Several attempts to prepare carbazole-based polymers have been conducted, which reveal and some interesting properties such as efficient energy harvest and transfer.<sup>14</sup> For example, the dendrimer with carbazole-based monodendrons synthesized by Zhao and co-workers displays stable green electroluminescent emission.<sup>15</sup> Zhang and coworkers also demonstrate that the dendrimer consisting of carbazole-based dendrons and the heterotriangulene cores have highly efficient energy transfer.<sup>16</sup>

The present work was undertaken to design and synthesize novel dendrimers consisting of 9-phenylcarbazole-based dendrons and triphenylamine core with precisely controlled generation of dendrons, in which the electron-rich triphenylamine was chosen as core because of its high p-type charge transport mobility and low ionization potential.<sup>17</sup> The bulky and twisted dendrons afford the dendrimer high steric hindrance which effectively inhibits the close molecular packing. Moreover, the large distortion angle of carbazole-based dendrons with respect to the triphenylamine core will interrupt the delocalization of  $\pi$ -electrons within the dendrimer so that the high triplet energy transition between carbazole and triphenylamine in the dendrimers is unperturbed, and the extent can be tuned through changing the generation. The effects of systematical variations of chemical and topological structures

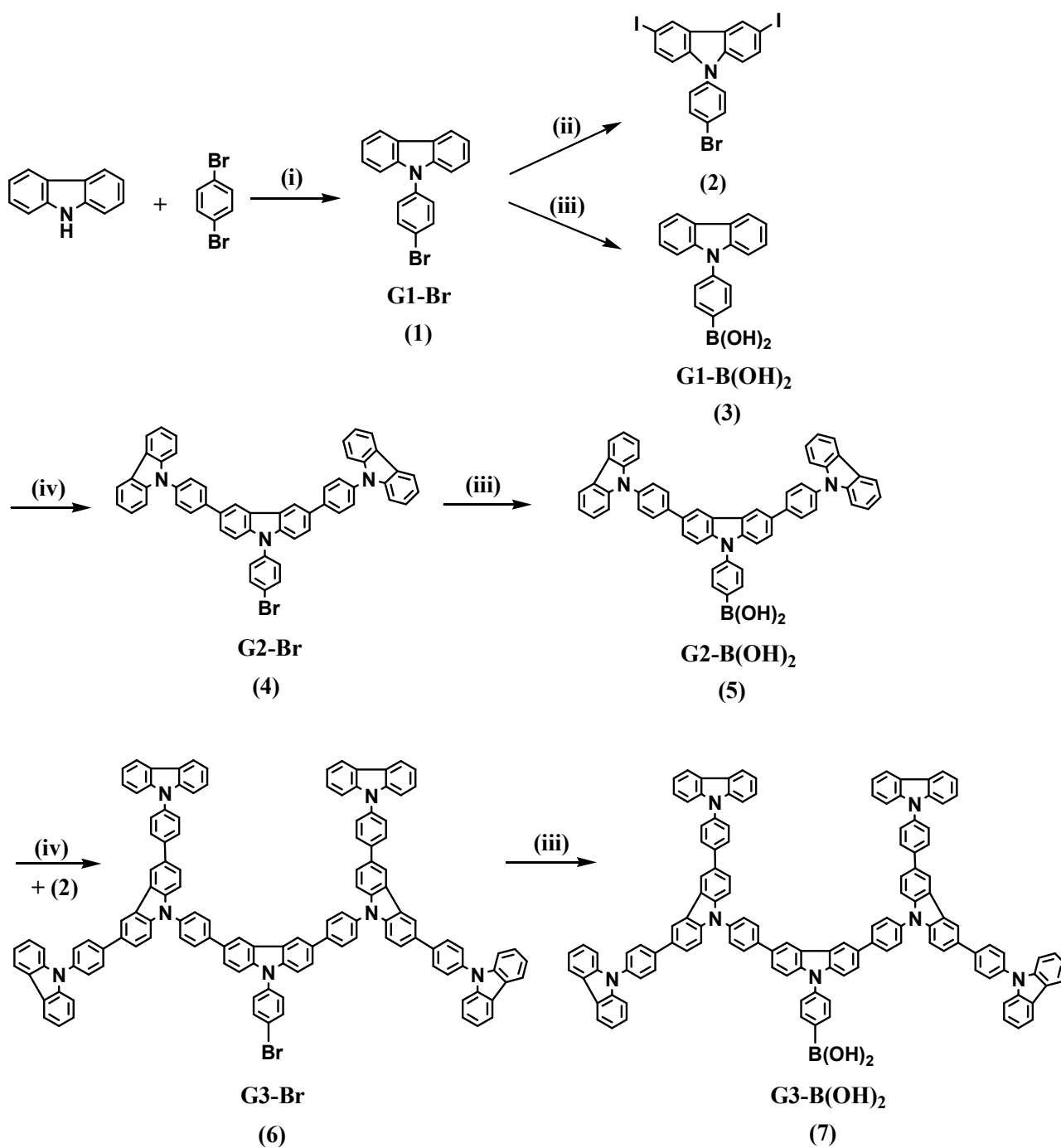
[View Online](#)

on thermal stability, photophysical and electrochemical properties of dendrimers of different generation numbers, e.g., quantum efficiencies, charge transports and HOMO-LUMO energy band gaps, will be investigated and discussed in detail.

## Results and Discussion

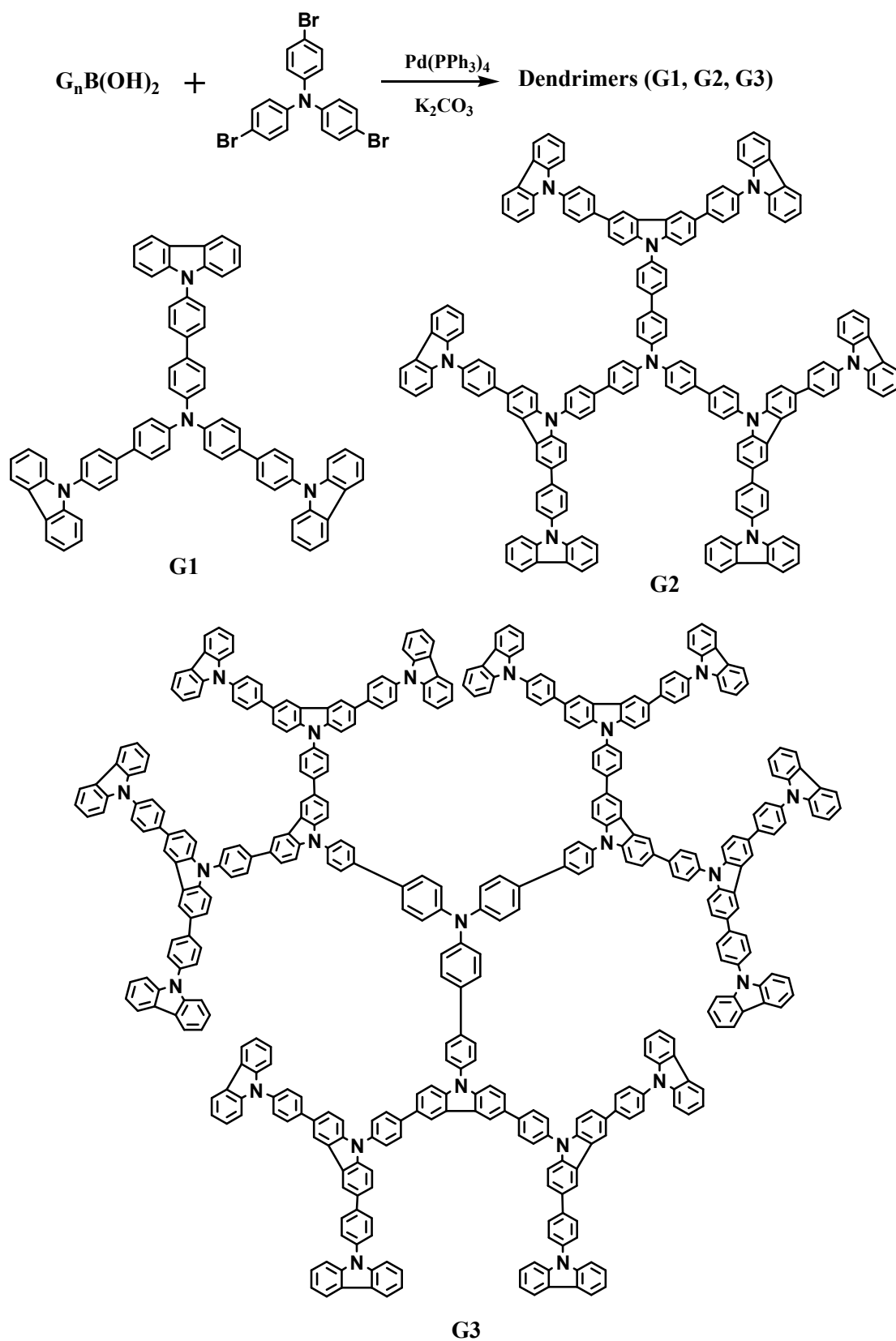
### Synthesis and characterization

The synthesis routes of 1st-3rd generations of dendrons,  $G_n\text{-B(OH)}_2$  ( $n = 1, 2, 3$ ) are outlined in Scheme 1. 9-(4-Bromophenyl)carbazole G1-Br (**1**) was synthesized from carbazole and 1,4-dibromobenzene by Ullmann coupling reaction. Iodination of G1-Br (**1**) at the 3, 6-positions using potassium iodide and potassium iodate in boiling glacial acetic acid led to diiodide (**2**) in good yield. The obtained G1-Br (**1**) was further reacted with *n*-BuLi in THF at  $-78\text{ }^\circ\text{C}$ , followed by the addition of triisopropyl borate, and hydrolysis with 2N HCl to give the corresponding 1st-generation dendron G1-B(OH)<sub>2</sub> (**3**). The Suzuki coupling of G1-B(OH)<sub>2</sub> (**3**) and (**2**) in the presence of tetrakis(triphenylphosphine) palladium and K<sub>2</sub>CO<sub>3</sub> gave G2-Br (**4**), which was then converted into the corresponding 2nd-generation dendron G2-B(OH)<sub>2</sub>. Similarly, G2-B(OH)<sub>2</sub> (**5**) was firstly coupled with (**2**) to afford G3-Br (**6**), and then converted into the 3rd-generation dendron G3-B(OH)<sub>2</sub> (**7**). Subsequently, the target dendrimers (**G1**, **G2** and **G3**) were synthesized by Suzuki coupling of corresponding 1st-3rd generations of dendrons with tris(4-bromophenyl)amine, using toluene/water system in the presence of tetrakis(triphenylphosphine) palladium, K<sub>2</sub>CO<sub>3</sub> and tricapyrylmethylammonium chloride, respectively (Scheme 2).



**Scheme 1.** Synthesis of 9-phenylcarbazole based dendrons,  $G_n-B(OH)_2$  ( $n = 1, 2, \text{ and } 3$ )<sup>a</sup>

<sup>a</sup> Reagents and conditions: (i)  $CuI$ ,  $K_2CO_3$ , 18-Crown-6, DMPU,  $170\text{ }^\circ C$ , 11h; (ii)  $KI$ ,  $KIO_3$ , acetic acid, reflux, 4h; (iii) (a)  $nBuLi$ , THF,  $-78\text{ }^\circ C$ , 1h, (b)  $(iPrO)_3B$ ,  $-78\text{ }^\circ C$ , 1h; (iv)  $Pd(PPh_3)_4$ ,  $K_2CO_3$ , Toluene,  $50\text{ }^\circ C$ , overnight.



Scheme 2. Synthesis of dendrimers (G1, G2, G3)

The chemical structures of dendrons were confirmed by the  $^1\text{H}$  NMR (Fig. S1-S6, Supporting Information) and elemental analysis. For G2-Br, the appearance of only a single peak at 8.55 ppm indicates that G1-B(OH) $_2$  has reacted completely with 3,6-diiodo-9-(4-bromophenyl)carbazole (**2**) (Fig. 1S). In the spectrum of G3-Br (Fig. 3S), the peaks at 8.59 ppm is assigned to the proton-i from G2-B(OH) $_2$ , whereas that at 8.62 ppm is attributed to proton-p from 3,6-diiodo-9-(4-bromophenyl)carbazole, indicative of the successful coupling reaction. After conversion of bromine atoms into boronic acid groups, relative to G2-Br and G3-Br, the chemical shifts of proton-j and k in G2-B(OH) $_2$  and G3-B(OH) $_2$  shift apparently to low field, respectively (Fig. 2S and 4S). The measured results by elemental analysis of the dendrons agree to their theoretical values.

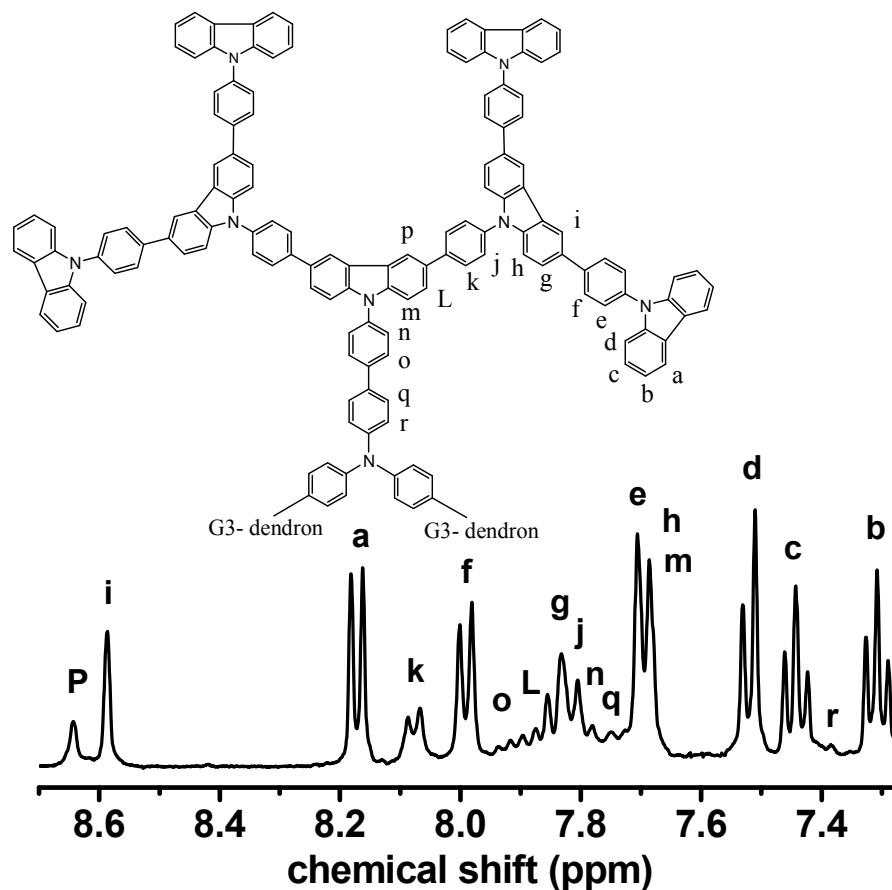
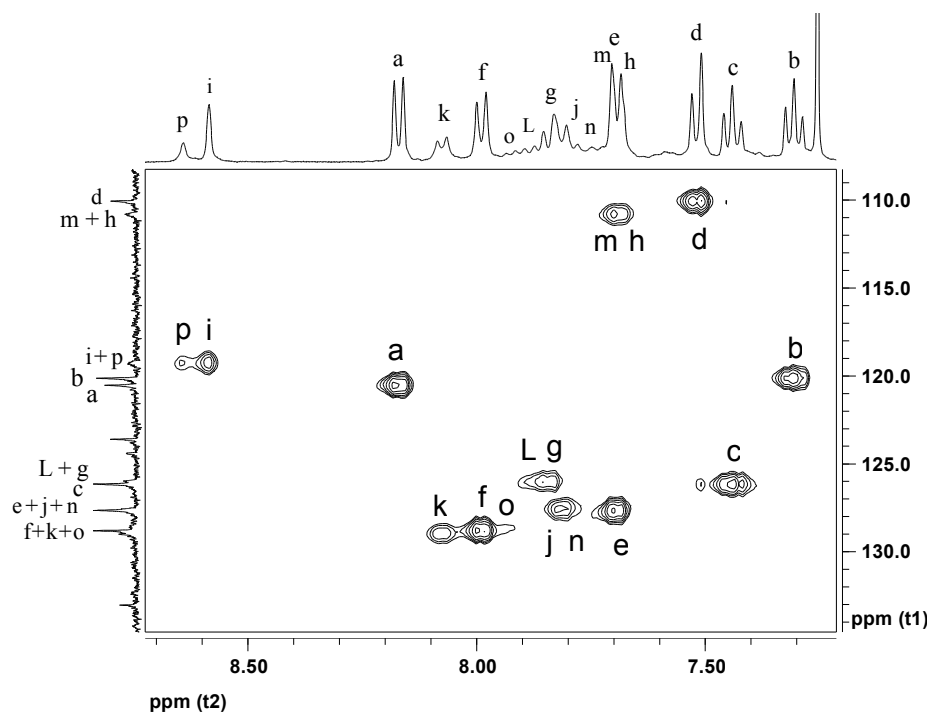


Fig. 1  $^1\text{H}$  NMR spectrum of G3 in chloroform-d (400 MHz).



assigned. In this regard, the two-dimensional H-H COSY and C-H HSQC spectra were measured. According to the H-H COSY (Fig. 2), the singlet at 8.58 ppm is correlated to a signal at 7.83 ppm, whereas the signal at 7.83 ppm is correlated to that at 7.69 ppm. The peak at 8.58 ppm has been assigned to the proton-i. Therefore, the signals at 7.83 and 7.69 ppm are attributed to the proton-g and h, respectively. In addition, other chemical shifts at 8.18 ppm (proton-k), 7.93 ppm (proton-o), 7.91 ppm (proton-l) and 7.74 ppm (proton-q) are also correlated to the signals at 7.82 ppm (proton-j), 7.72 ppm (proton-n), 7.69 ppm (proton-m) and 7.38 ppm (proton-r), respectively. Furthermore, the C-H HSQC spectrum in Fig. 3 reveals the following C-H correlated signals: carbon resonances at 111.0 ppm for h (7.68/111.0 ppm) and m (7.67/111.0 ppm), at 119.0 ppm for i (8.58/119.0 ppm) and p (8.64/119.0 ppm), at 126.0 ppm for g (7.83/126.0 ppm) and l (7.88/126.0 ppm), at 127.5 ppm for e (7.69/127.5 ppm), j (7.80/127.5 ppm) and n (7.78/127.5 ppm), and at 128.5 ppm for f (7.99/128.5 ppm), k (8.07/128.5 ppm) and o (7.92/128.5 ppm). Based on the H-H COSY and C-H HSQC results, all the signals in Fig. 1 are well assigned the corresponding protons in dendrimer **G3**.



**Fig. 3** C-H HSQC spectrum of **G3** in chloroform-d (400 MHz).

[View Online](#)

In addition, MALDI-TOF mass spectrometry for each dendrimer was performed to provide the definite evidences for the structures of dendrimers (Fig. 4). For the three generations of dendrimers, the determined molecular weights are well consistent with the proposed structures. For example, according to the molecular formula of  $C_{396}H_{246}N_{22}$  (**G3**), the calculated molecular weight of  $[M + Na]^+$  is 5334.34, while the corresponding sharp single peak in the MALDI-TOF spectrum appears at 5334.95.

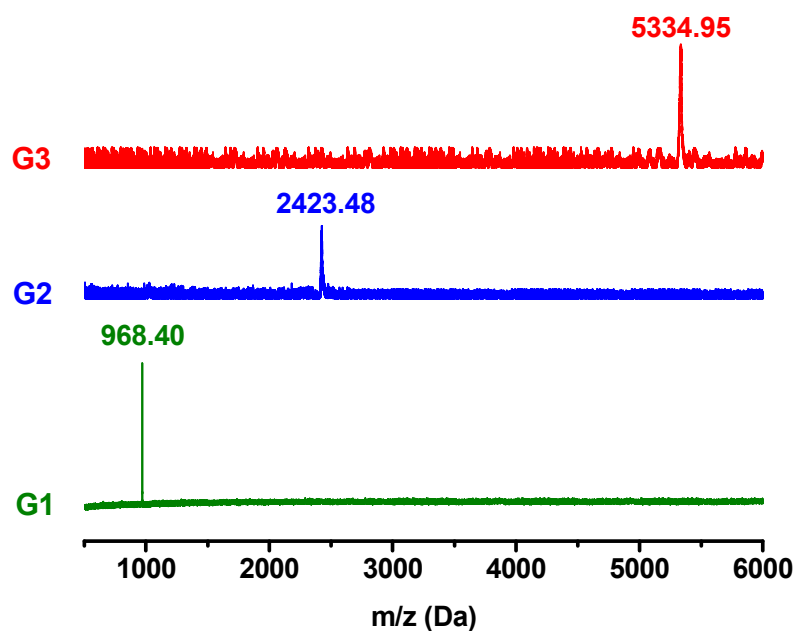


**Fig. 4** MALDI-TOF-MS spectra of dendrimers **G1-G3**.

The thermal stabilities of **G1-G3** were evaluated by thermogravimetric analysis (TGA) under nitrogen atmosphere. As illustrated in Fig. 5, all the dendrimers exhibit excellent thermal stability with 5 % weight-loss temperatures ( $T_{5\%}$ ) over 540 °C. Moreover, both the  $T_{5\%}$  values and residual weights at 850 °C show apparent increases with the generation of the dendrimer, indicating that the incorporation of 9-phenylcarbazole is advantageous for the resistance to heat. In addition, in contrast to **G1** and **G2**, **G3** displays two-step degradations, locating at around 576 °C and 652 °C, respectively, suggesting that, for the higher-generation dendrimer, the thermal cleavage firstly occurs in the outermost layer, and then the internal dendrons and core start to decompose.

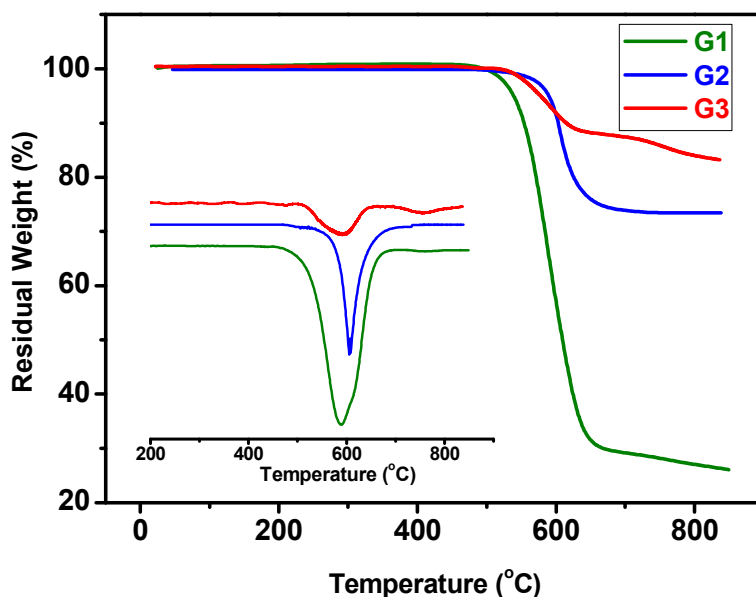


Fig. 5 TG and DTG traces of dendrimers measured at a heating rate of  $10\text{ }^{\circ}\text{C min}^{-1}$ .

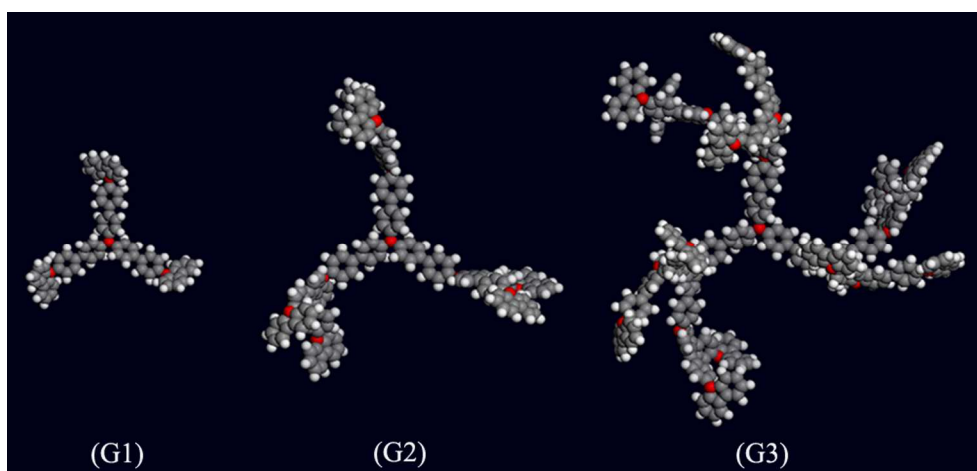
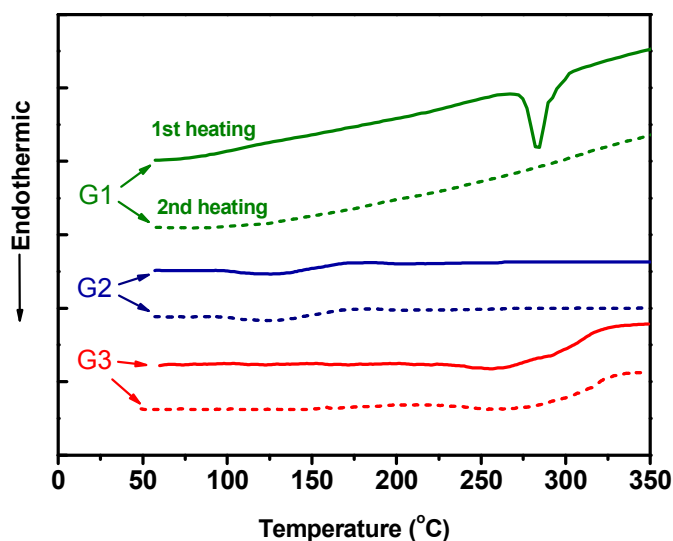


Fig. 6 Computer simulations for the dendrimers G1-G3.

In order to elucidate the effects of growth of generation on the crystalline behavior, photophysical and electrochemical properties, computer modeling was carried out to reveal information of the conformation and topology of the dendrimers using Materials Studio Modeling Software. Molecular models were energy minimized via conjugate-gradient method. The algorithm was set to Polak-Ribiere, and the convergence and line search were equal to 0.1 and 0.5, respectively. After successive geometry

[View Online](#)

and molecular mechanics optimizing, the energy-minimized structures are relaxed through dynamic calculation at 298 K for 200 ps based on the COMPASS force field to obtain the molecular models as illustrated in Fig. 6. Each dendrimer is constructed with three identical 9-phenylcarbazole-based dendrons symmetrically stretched from the triphenylamine core. However, the presence of the torsional angle between the benzene-carbazole rings and bending angle of C-N-C bond gives rise to the dendrimers greatly contorted structures, and the twisted extent is more pronounced for the dendrimer of higher generation. For the 3rd-generation dendrimer, the bulky dendron becomes almost perpendicular to the benzene ring owing to the increased steric hindrance and molecular internal tension.



**Fig. 7** DSC curves of dendrimers **G1-G3** for the first heating run (solid line) and second heating run (dashed line).

The twisted extent and the size of the dendron significantly affect the aggregation structure of dendrimer molecules. The DSC curves in Fig. 7 show that the bulky and distortional dendrons lead to the dendrimer greatly decreased crystalline ability. For example, in the first heating curve, no any melting peak can be detected for the 2nd and 3rd-generation dendrimers (**G2** and **G3**), indicating that **G2** and **G3** are amorphous in nature. On the contrary, the 1st-generation dendrimer (**G1**) displays a sharp crystalline peak at 283 °C. It is noteworthy that, even though **G1** can crystallize under some

conditions, its crystalline ability is rather limited because its molecule also twists to some extent and is rather rigid. As a result, when the melting **G1** is fast cooled to room temperature and then reheated for the second DSC run, the former crystalline peak completely disappears, showing that the melt can not rapidly crystallize in the course of quenching treatment.

In addition, in the second heating DSC curves, **G2** and **G3** show glass transition temperatures at 150 and 270 °C, respectively. Relative to **G2**, the remarkably higher  $T_g$  value for **G3** means that the incorporation of carbazole unit and large dendron can effectively increase the steric hindrance and rigidity of the dendrimer.

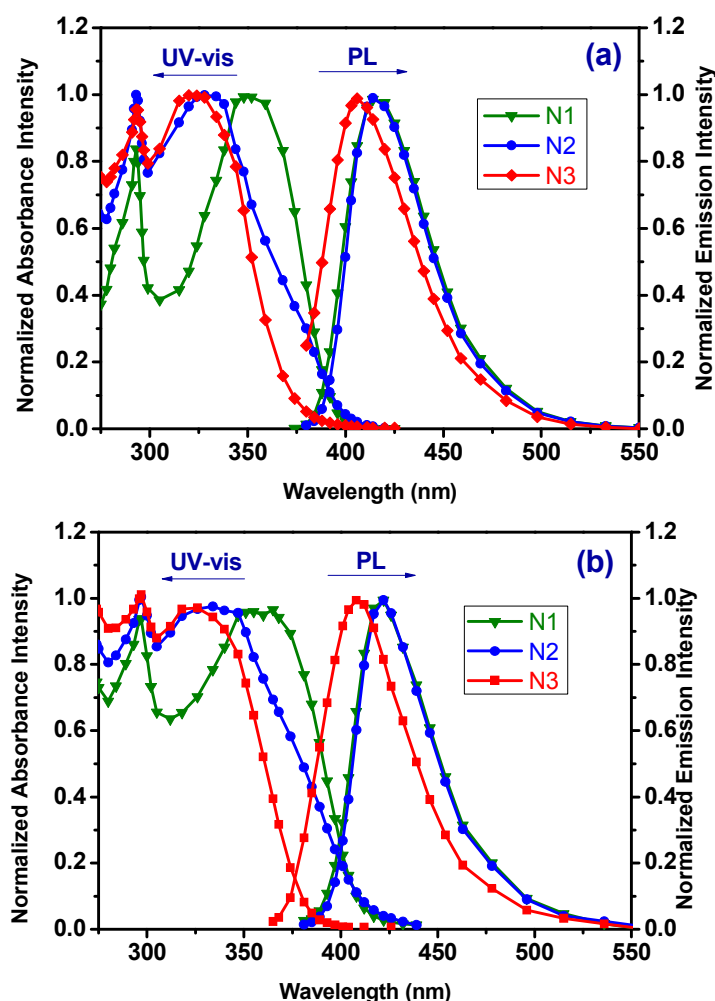


**Fig. 8** UV-vis and PL spectra of dendrimers (a) THF solutions and (b) solid films.

### Photophysical properties of solution and film sample of dendrimers

[View Online](#)

The optical properties of the dendrimers in both solution and solid state were investigated by UV-vis absorption and photoluminescence (PL) spectroscopy. The UV absorption and fluorescence spectra with normalized peak intensities are presented in Fig. 8, and the photophysical data are summarized in Table 1. For the **G1** solution sample (Fig. 8a), the UV absorption band at 293 nm is attributed to the absorption of triphenylamine core,<sup>18</sup> whereas that at 317-350 nm comes from the N-phenylcarbazole-based dendron.<sup>19</sup> With the increase of generation, the band positions at 293 nm corresponding to triphenylamine core for **G2** and **G3** remain almost the same as that of **G1**, but the intensities are apparently increased owing to the efficient conjugation from the dendrons.<sup>20</sup> On the other hand, relative to **G1**, the former absorption band belonging to the dendron is remarkably blue shifted from 350 nm to 328 nm for **G2** and 322 nm for **G3**. The reason can be attributed to the reduced  $\pi$ -conjugation of the N-phenylcarbazole-based dendron caused by the increase of twisted extent with the generation.

**Table 1** Photophysical data of dendrimers G1-G3

dendrimer	Abs (nm)		PL (nm)		$\Phi_{\text{PL}}$ (%) <sup>d</sup>	Band gap (eV) <sup>e</sup>
	Solution <sup>a</sup> ( $\epsilon \times 10^5$ ) <sup>b</sup>	film <sup>c</sup>	Solution <sup>a</sup>	film <sup>c</sup>		
G1	350 (3.8), 293 (4.4)	359, 296	416	420	64	2.90
G2	328 (5.5), 293 (5.5)	330, 296	414	421	88	2.84
G3	322 (4.6), 293 (4.8)	323, 296	406	408	95	3.15

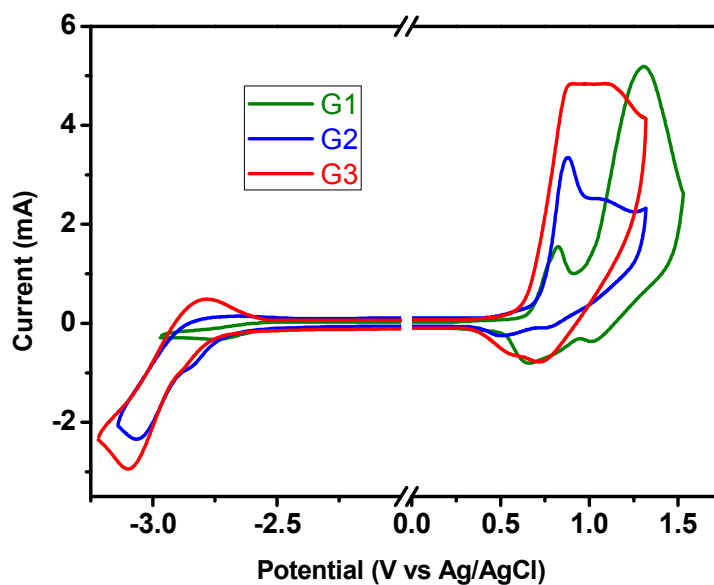
<sup>a</sup> Measured in THF solution at room temperature. <sup>b</sup> Mole absorption coefficient ( $\epsilon$ ):  $\text{M}^{-1} \text{cm}^{-1}$ , within an error of  $\pm 0.1 \times 10^5 \text{M}^{-1} \text{cm}^{-1}$ . <sup>c</sup> Measured in solid-state film. <sup>d</sup> Fluorescence quantum efficiency measured in THF using quinine sulfate dihydrate as a standard.<sup>21</sup> <sup>e</sup> Band gaps were calculated from the onsets of UV-visible absorption spectra of **G1-G3** in solid films

The comparison of Fig. 8a and 8b reveals that the solution and solid film samples display the very similar UV absorption profiles and positions of bands for both the triphenylamine core and 9-

phenylcarbazole-based dendrons, indicating that the molecular conformations of the dendrimers do not apparently change in both states, and the intermolecular aggregation has been significantly suppressed by the rigid, bulky and twisted dendrons.<sup>22</sup> According to the onset positions of UV absorptions of 427 nm, 436 nm and 393 nm for **G1**, **G2** and **G3**, the band gaps of dendrimers were calculated and the values are 2.90, 2.84 and 3.15 eV, respectively. Relative to **G1**, with the growth of generation, the band gap initially displays a slight decrease (**G2**), and then significantly increases (**G3**). The possible reasons for this phenomenon can be due to the synergistic effect of two opposing factors. Generally, the enlarged dendron based on carbazole is advantageous for the  $\pi$ -conjugative effect, resulting in a decreased band gap of the dendrimer. On the other hand, as revealed by the computer simulation, with the growth of generation, the bulky dendrons become greatly twisted, which gives rise to increased band gap. For **G3**, the later factor plays the major role.

Photoluminescence spectra of the dendrimers, excited at 370nm, in THF solution at a concentration of  $5 \times 10^{-5}$  M and in thin neat films are shown in Fig. 8. The fluorescence emission spectra of three solution samples display emissions at 416, 414 and 406 nm for **G1**, **G2** and **G3**, respectively. It is observed that, compared to **G1** and **G2**, the emission peak of **G3** apparently blue-shifts. The solid films exhibit the similar PL spectra to the solution samples, indicating that the rigid dendrons and non-planar triphenylamine core can prevent the molecules from aggregation.<sup>23</sup> In addition, the full-width at half-maximum of emission spectra (FWHM) of the dendrimers are found to be only around 47-49 nm in solutions and 46-50 nm in the solid films, implying that these dendrimers are suitable for donors that transfer energy to fluorophores with lower band gap in EL devices.<sup>24</sup>

The quantum yields of the dendrimers measured in dilute solution using quinine sulfate as a reference are 64, 88 and 95 % for **G1**, **G2** and **G3**, respectively, displaying significantly increased PL efficiencies with the generation of dendrimer. The reason may be that the high twisting extent and reduced  $\pi$ -electron conjugation of dendrons are advantageous for the decrease of energy wastage for charge transfer and nonradiative decay.

[View Online](#)

**Fig. 9** Cyclic voltammograms of thin films of dendrimers in 0.1 M anhydrous acetonitrile solution of  $n\text{Bu}_4\text{NPF}_6$  at room temperature.

### Electrochemical behavior of dendrimers

The electrochemical properties of the dendrimers were investigated by cyclic voltammetry (CV). The measurements were conducted at room temperature under nitrogen. The films of dendrimers obtained by drop-casting of dendrimer solution on glassy carbon electrode were used as the working electrode, and an  $\text{Ag}/\text{Ag}^+$  electrode was used as the reference electrode, which was calibrated using the ferrocene/ferrocenium ( $\text{Fc}/\text{Fc}^+$ ) redox couple (4.8 eV below the vacuum level) prior to use.<sup>25</sup> As shown in Fig. 9, **G1** displays two electrochemical oxidation peaks, meaning that there are two independent oxidation potentials. The first one is assigned to the oxidation of triarylamine core and the second redox to the carbazole dendrons.<sup>24</sup> In addition, it is observed that, with the increase of generation, the redox couples of dendrimers shift to lower potentials, and meanwhile, the first redox wave corresponding to the oxidation potential of dendron is overlapped with the anodic redox one of the triphenylamine core.<sup>26</sup> Upon the cathodic scanning, the reduction process of **G1** and **G2** are irreversible, but the reduction potential of **G3** becomes reversible, suggesting that **G1** and **G2** are more favorable for oxidation (p-

doping) rather than reduction (n-doping), whereas **G3** is sufficiently stable and suitable for both hole and electron injections.

**Table 2** Cyclic voltammogram data of dendrimers G1-G3

dendrimer	$E_{\text{onset(ox)}} \text{ (V)}^{\text{a}}$	$E_{\text{onset(red)}} \text{ (V)}^{\text{a}}$	HOMO (eV) <sup>b</sup>	LUMO (eV) <sup>b</sup>	$E_{\text{g}} \text{ (eV)}^{\text{c}}$
G1	0.60	-2.54	-5.40	-2.26	3.14
G2	0.58	-2.56	-5.38	-2.24	3.14
G3	0.56	-2.60	-5.36	-2.20	3.16

<sup>a</sup> Onset oxidation and reduction potentials versus Ag/Ag<sup>+</sup> (0.01 V); <sup>b</sup> estimated from the onset oxidation and reduction potential by using HOMO =  $-E_{\text{onset(ox)}} - 4.8 \text{ eV}$  and LUMO =  $-E_{\text{onset(red)}} - 4.8 \text{ eV}$ ; <sup>c</sup> Electrochemical band gaps determined using  $E_{\text{g}} = E_{\text{onset(ox)}} - E_{\text{onset(red)}}$ .<sup>27</sup>

On the other hand, Table 2 shows that the first oxidation potentials ( $E_{\text{onset(ox)}}$ ) of **G1**, **G2** and **G3** are 0.60, 0.58 and 0.56 eV, respectively, indicating that synergistic effect of the 9-phenyl carbazole-based dendrons and the triphenylamine core results in outstanding electron-donating capacities. Moreover, the  $E_{\text{onset(ox)}}$  values of dendrimers are shifted negatively with the increase of generation from **G1** to **G3**, which is also attributed to the increasing content of electron-rich carbazole moieties. The highest occupied molecular orbitals (HOMO) and lowest unoccupied molecular orbitals (LUMO) of the dendrimers were calculated from the following equations: HOMO =  $-E_{\text{onset(ox)}} - 4.8 \text{ eV}$ , and LUMO =  $-E_{\text{onset(red)}} - 4.8 \text{ eV}$ . Accordingly, for **G1**, **G2** and **G3**, the HOMO energy levels are -5.40, -5.38 and -5.36 eV, and the LUMO energy levels are -2.26, -2.24 and -2.20 eV, respectively. As can be seen, the HOMO energy levels of these dendrimers are in the range from -5.40 to -5.36 eV, very close to the work function of the ITO (indium tin oxide)/PEDOT (poly(3,4-ethylenedioxythiophene)) electrode (work function -5.2 eV).<sup>28</sup> This characteristics is especially beneficial to the efficient hole injection and transport for optoelectronic materials. In addition, from the equation of  $E_{\text{g}} = E_{\text{onset(ox)}} - E_{\text{onset(red)}}$ , the

[View Online](#)

obtained band gaps ( $E_g$ ) of **G1** and **G2** are 3.14 eV, whereas the value for **G3** slightly increases to 3.16 eV, which is consistent with the blue-shifting trend observed in the PL spectra of dendrimers.

## Conclusions

We have successfully synthesized three dendrimers with various generations (**G1**, **G2**, **G3**) consisting of a triphenylamine core and 9-phenylcarbazole based dendrons through the convergent approach. Their chemical structures were well characterized. All the dendrimers exhibit the 5% weight loss temperature over 540 °C. The 3rd-generation dendrimer has the  $T_g$  value of 270 °C, which is the highest among them. The solution and solid samples have very similar UV absorption and fluorescence emission profiles, indicating that the intermolecular aggregation has been greatly suppressed by the rigid, bulky and twisted dendrons as revealed by the computer modeling results. As a result, the dendrimers display narrow emission band, and with the generation growth, the quantum yields significantly increase from 63.8 % of **G1** to 95.4 % of **G3**. In addition, CV measurements show that the dendrimers have a gradient change for the HOMO and energy band gap with the incremental dendrons. The HOMO levels of dendrimers are in the range from -5.43 to -5.36 eV, very close to the HOMO energy of PEDOT:PSS ((3,4-polyethylenedioxythiophene) poly(styrenesulfonate)) (work function -5.2 eV). This characteristic is very beneficial for hole-transporting and injection materials. The combination of excellent thermal stability, excellent luminescent properties and the capacity of tuning the hole-transporting properties renders the dendrimers promising potential in OLED field.

## Experimental

### Materials

Tris(4-bromophenyl)amine, 1,4-dibromobenzene, carbazole, tetrakis(triphenylphosphine)palladium, *n*BuLi and triisopropyl borate were purchased, and used without further purification. THF was freshly distilled from sodium/benzophenone prior to use. Other commercial reagents were of analytical grade

and used as received unless otherwise stated. All chromatographic separations were carried out on silica gel (400 mesh).

### Instrumentation

Conventional  $^1\text{H}$  NMR as well as two-dimensional H-H Correlation Spectroscopy (COSY) and C-H correlated Heteronuclear Single Quantum Coherence (HSQC) spectra were measured on a Varian INOVA at 400 MHz with  $\text{CDCl}_3$  as solvent and tetramethylsilane as internal standard.

Molecular masses were measured on a MALDI micro MX laser desorption-ionization time-of-flight mass spectrometer (MALDI-TOF MS). Samples were analyzed using a THF solution of the sample (3  $\mu\text{L}$ ) mixed with 3  $\mu\text{L}$  of dithranol matrix (25 mg  $\text{mL}^{-1}$  in THF) before loading onto a metal sample plate.

Elemental analyses were determined with an Elementar Vario EL III elemental analyzer.

Thermal gravimetric analyses (TGA) were carried out on a NETZSCH TG209C under nitrogen atmosphere at a heating rate of  $10\text{ }^\circ\text{C min}^{-1}$ .

Different scanning calorimetries (DSC) were performed on a NETZSCH DSC204 with a heating rate of  $10\text{ }^\circ\text{C min}^{-1}$  under nitrogen atmosphere.

UV absorption and photoluminescence (PL) spectra were performed on a HP-8453 spectrophotometer and a PTI-700 luminescence spectrometer, respectively.

Cyclic voltammeteries (CV) were determined on a BSA 100B electrochemical analyzer with a conventional three-electrode configuration consisting of a glassy carbon working electrode, a platinum auxiliary electrode and a non-aqueous  $\text{Ag}/\text{AgNO}_3$  reference electrode.

### Synthesis

**Synthesis of 4-Carbazolyl-1-bromobenzene, G1-Br (1).** The synthesis of 4-carbazolyl-1-bromobenzene was carried out in the procedure described in the literature with some modifications.<sup>27</sup> A mixture of  $\text{CuI}$  (1.14 g, 6 mmol), 18-Crown-6 (0.53 g, 2 mmol),  $\text{K}_2\text{CO}_3$  (16.6 g, 120 mmol), 1,3-dimethyl-3,4,5,6-tetrahydro-2(1H)-pyrimidinone (DMPU) (2 mL), 1,4-dibromobenzene (14.2 g, 60 mmol) and carbazole (10 g, 60 mmol) was stirred at  $170\text{ }^\circ\text{C}$  for 11 h under nitrogen. After cooling to

[View Online](#)

room temperature, it was poured into 150 mL 1 N-HCl aqueous solution. The precipitate was filtered and successively washed with  $\text{NH}_3\text{H}_2\text{O}$  and deionized water. The solid was further purified with column chromatography using hexane as eluant to afford a white solid. Yield 71% (11.7 g, 0.036 mol); m.p. 152-153 °C;  $^1\text{H}$  NMR (400 MHz,  $\text{CDCl}_3$ ):  $\delta$ =8.13 (d,  $^3\text{J}(\text{H},\text{H}) = 7.6$  Hz, 2 H; Ar-H), 7.72 (d,  $^3\text{J}(\text{H},\text{H}) = 8.8$  Hz, 2 H; Ar-H), 7.45 (d,  $^3\text{J}(\text{H},\text{H}) = 8.8$  Hz, 2 H; Ar-H), 7.41–7.37 (dt,  $^3\text{J}(\text{H},\text{H})_1 = 6.8$  Hz,  $^3\text{J}(\text{H},\text{H})_2 = 6.8$  Hz, 4H; Ar-H), 7.30 ppm (t,  $^3\text{J}(\text{H},\text{H}) = 6.6$  Hz, 2H; Ar-H); elemental analysis calcd (%) for  $\text{C}_{18}\text{H}_{12}\text{BrN}$ : C 67.10, H 3.75, N 4.35; found: C 67.21, H 3.70, N 4.29.

**Synthesis of 3,6-Diiodo-9-(4-bromophenyl)carbazole (2).** 3,6-diiodo-9-(4-bromophenyl)carbazole was prepared according to the procedure described previously.<sup>29</sup> 4-Carbazolyl-1-bromobenzene (0.65 g, 2 mmol) was dissolved in boiling glacial acetic acid (40 mL), and then potassium iodide (0.66 g, 3.96 mmol) and potassium iodate (0.96 g, 4.5 mmol) were added. After reacting at the refluxing temperature under the protection of nitrogen for 4 h, the mixture was poured into 150 mL water, and the precipitate was filtered and washed successively with water. The product was purified by recrystallization from chloroform/ethanol to afford a white solid. Yield 85% (3.64 g, 6.3 mmol); m.p. 239-241 °C;  $^1\text{H}$  NMR (400 MHz,  $\text{CDCl}_3$ ):  $\delta$ =8.38 (s, 2H; Ar-H), 7.74(d,  $^3\text{J}(\text{H},\text{H}) = 8.8$  Hz, 2H; Ar-H), 7.67(d,  $^3\text{J}(\text{H},\text{H}) = 8.8$  Hz, 2H; Ar-H), 7.37(d,  $^3\text{J}(\text{H},\text{H}) = 8.2$  Hz, 2H; Ar-H), 7.11 ppm (d,  $^3\text{J}(\text{H},\text{H}) = 8.8$  Hz, 2H; Ar-H); elemental analysis calcd (%) for  $\text{C}_{18}\text{H}_{10}\text{BrI}_2\text{N}$ : C 37.66, H 1.76, Br 13.92, I 44.22, N 2.44; found: C 37.56, H 1.80, Br 13.84, I 44.31, N 2.40.

**Synthesis of 4-carbazolyl-1-phenylboronic acid, G1-B(OH)<sub>2</sub> (3).** 4-Carbazolyl-1-phenylboronic acid was prepared according to a similar method described in the literature<sup>28</sup> with some modifications. 7.2 mL of 2.5 M *n*BuLi (18 mmol) in hexane was added dropwise to a solution of 4-carbazolyl-1-bromobenzene (4.3 g, 15 mmol) in THF (40 mL) at -78 °C. After stirring for 1h, triisopropyl borate (32 mL, 18 mmol) was added using a syringe. The reaction mixture was reacted for additional 1 h and then was warmed slowly to room temperature and stirred overnight. The supernatant was diluted with ether

(100 mL) and washed with water. The organic layer was dried over  $\text{MgSO}_4$ , and the solution was concentrated using a rotary evaporator. The solid was further purified with column chromatography using a mixture of hexane and ethyl acetate as a gradient eluent to afford a white solid. Yield 87% (3.3 g, 0.011 mol); m.p. 262-264 °C;  $^1\text{H NMR}$  (400 MHz,  $\text{CDCl}_3$ ):  $\delta$  = 8.56 (d,  $^3\text{J}(\text{H,H}) = 8.0$  Hz, 2H; Ar-H), 8.18 (d,  $^3\text{J}(\text{H,H}) = 7.6$  Hz, 2H; Ar-H), 7.80 (d,  $^3\text{J}(\text{H,H}) = 8.0$  Hz, 2H; Ar-H), 7.56 (d,  $^3\text{J}(\text{H,H}) = 8.0$  Hz, 2H; Ar-H), 7.46 (t,  $^3\text{J}(\text{H,H}) = 7.2$  Hz, 2H; Ar-H), 7.33 ppm (t,  $^3\text{J}(\text{H,H}) = 7.6$  Hz, 2H; Ar-H); elemental analysis calcd (%) for  $\text{C}_{18}\text{H}_{14}\text{BNO}_2$ : C 75.30, H 4.91, N 4.88; found: C 75.36, H 4.82, N 4.81.

**Synthesis of 4-[3', 6'-Di(4'-Carbazolylbenzene-1'-yl)carbazolyl]-1-bromobenzene, G2-Br (4).**

4-[3', 6'-Di(4'-carbazolylbenzen-1'-yl)carbazolyl]-1-bromobenzene was prepared in the procedure described in the literature with some modifications.<sup>30</sup> To a mixture of G1-B(OH)<sub>2</sub> (495 mg, 1.72 mmol), 3,6-diiodo-9-(4-bromophenyl)carbazole (449 mg, 0.78 mmol), and tetrakis(triphenylphosphine)-palladium (18 mg), toluene (30 mL) and 2 M  $\text{K}_2\text{CO}_3$  (4 mL) were charged into a 100 mL-round-bottom flask equipped with a magnetic stirrer, a  $\text{N}_2$  inlet and a reflux condenser. The system was heated to 50 °C and stirred at this temperature overnight. Then the mixture was poured into water which was extracted with chloroform three times. The combined organic layer was dried with anhydrous  $\text{Na}_2\text{SO}_4$ , filtered, and evaporated to dryness. The crude product was purified by silica gel column chromatography using petroleum ether/ $\text{CHCl}_2$  as an eluent to afford an orange solid. Yield 91% (0.571 g, 0.71 mmol); m.p. >300 °C;  $^1\text{H NMR}$  (400 MHz,  $\text{CDCl}_3$ ):  $\delta$  = 8.55 (s, 2H; Ar-H), 8.17 (d,  $^3\text{J}(\text{H,H}) = 8.0$  Hz, 4H; Ar-H), 7.97 (d,  $^3\text{J}(\text{H,H}) = 8.0$  Hz, 4H; Ar-H), 7.82 (m, 4H; Ar-H), 7.70 (d,  $^3\text{J}(\text{H,H}) = 8.4$  Hz, 4H; Ar-H), 7.57 (m, 4H; Ar-H), 7.52 (d,  $^3\text{J}(\text{H,H}) = 8.8$  Hz, 4H; Ar-H), 7.44 (t,  $^3\text{J}(\text{H,H}) = 7.2$  Hz, 4H; Ar-H), 7.30 ppm (t,  $^3\text{J}(\text{H,H}) = 7.2$  Hz, 4H; Ar-H); elemental analysis calcd (%) for  $\text{C}_{54}\text{H}_{34}\text{BrN}_3$ : C 80.59, H 4.26, N 5.22; found: C 80.51, H 4.33, N 5.14.

**Synthesis of 4-(3',6'-Di(4'-carbazolylbenzene-1'-yl)carbazolyl)phenylboronic Acid, G2-B(OH)<sub>2</sub> (5).**

The preparation procedure of G2-B(OH)<sub>2</sub> was similar to that of G1-B(OH)<sub>2</sub> except that the

[View Online](#)

precursor used was G2-Br instead of G1-Br. Yield 54% (0.43 g, 0.559 mmol); m.p. >300 °C; <sup>1</sup>H NMR (400 MHz, CDCl<sub>3</sub>): δ= 8.99 (s, 2H; Ar-H), 8.17 (m, 6H; Ar-H), 8.20 (m, 6H; Ar-H), 7.82 (d, <sup>3</sup>J(H,H) = 7.6 Hz, 2H; Ar-H), 7.83 (d, <sup>3</sup>J(H,H) = 8.8 Hz, 4H; Ar-H), 7.78 (d, 2H, <sup>3</sup>J(H,H) = 8.0 Hz, 2H; Ar-H), 7.66 (d, <sup>3</sup>J(H,H) = 7.6 Hz, 2H; Ar-H), 7.56-7.50 (m, 8H; Ar-H), 7.37 ppm (t, <sup>3</sup>J(H,H) = 6.4 Hz, 4H; Ar-H); elemental analysis calcd (%) for C<sub>54</sub>H<sub>36</sub>BN<sub>3</sub>O<sub>2</sub>: C 84.26, H 4.71, N 5.46; found: C 84.20, H 4.77, N 5.53.

**Synthesis of 9-(4-(6-(4-(3,6-Bis(4-(9H-carbazol-9-yl)phenyl)-9H-carbazol-9-yl)phenyl)-9-(4-bromophenyl)-9H-carbazol-3-yl)phenyl)-3,6-bis(4-(9H-carbazol-9-yl)phenyl)-9H-carbazole, G3-Br (6).** The preparation procedure of G3-Br was similar to that of G2-Br except that the precursor used was G2-B(OH)<sub>2</sub> instead of G1-B(OH)<sub>2</sub>. Yield 69% (0.32 g, 0.18 mmol); m.p. >300 °C; <sup>1</sup>H NMR (400 MHz, CDCl<sub>3</sub>): δ= 8.62 (s, 2H; Ar-H), 8.59 (s, 4H; Ar-H), 8.17 (d, <sup>3</sup>J(H,H) = 8.0 Hz, 8H; Ar-H), 8.06 (d, <sup>3</sup>J(H,H) = 8.4 Hz, 4H; Ar-H), 7.99 (d, <sup>3</sup>J(H,H) = 8.0 Hz, 8H; Ar-H), 7.88-7.81 (m, 12H; Ar-H), 7.71-7.68 (m, 12H; Ar-H), 7.59 (d, <sup>3</sup>J(H,H) = 8.8 Hz, 4H; Ar-H), 7.52 (d, <sup>3</sup>J(H,H) = 8 Hz, 8H; Ar-H), 7.45 (t, <sup>3</sup>J(H,H) = 7.6 Hz, 8H; Ar-H), 7.32 ppm (t, <sup>3</sup>J(H,H) = 7.2 Hz, 8H; Ar-H); <sup>13</sup>C NMR (CDCl<sub>3</sub>, 100MHz): δ= 141.2, 140.9, 136.2, 133.5, 132.8, 128.9, 128.6, 127.7, 127.5, 125.9, 124.4, 124.2, 123.4, 120.4, 120.0, 119.2, 110.6, 109.8 ppm; elemental analysis calcd (%) for C<sub>126</sub>H<sub>78</sub>BrN<sub>7</sub>: C 85.50, H 4.44, N 5.54; found, C 85.45, H 4.41, N 5.58.

**Synthesis of 4-(3,6-bis(4-(3,6-bis(4-(9H-carbazol-9-yl)phenyl)-9H-carbazol-9-yl)phenyl)-9H-carbazol-9-yl)phenylboronic Acid, G3-B(OH)<sub>2</sub> (7).** The preparation procedure of G3-B(OH)<sub>2</sub> was similar to that of G2-B(OH)<sub>2</sub> except that the precursor used was G3-Br instead of G2-Br. Yield 50% (0.27 g, 0.156 mmol); m.p. >300 °C; <sup>1</sup>H NMR (400 MHz, CDCl<sub>3</sub>): δ= 8.62 (s, 2H; Ar-H), 8.59 (s, 4H; Ar-H), 8.17 (d, <sup>3</sup>J(H,H) = 8.0 Hz, 8H; Ar-H), 8.07 (d, <sup>3</sup>J(H,H) = 8.4 Hz, 4H; Ar-H), 7.99 (d, <sup>3</sup>J(H,H) = 8.0 Hz, 8H; Ar-H), 7.87-7.76 (m, 12H; Ar-H), 7.71-7.63 (m, 16H; Ar-H), 7.52 (d, <sup>3</sup>J(H,H) = 8.4 Hz, 8H; Ar-H), 7.45 (t, <sup>3</sup>J(H,H) = 7.6 Hz, 8H; Ar-H), 7.31 ppm (t, <sup>3</sup>J(H,H) = 7.6 Hz, 8H; Ar-H); <sup>13</sup>C NMR

(CDCl<sub>3</sub>, 100MHz):  $\delta$  = 141.1, 140.9, 136.3, 132.9, 128.6, 127.3, 126.0, 124.1, 123.4, 120.4, 119.9, 118.9, 110.6, 109.8 ppm; elemental analysis calcd (%) for C<sub>126</sub>H<sub>80</sub>BN<sub>7</sub>O<sub>2</sub>: C 87.23, H 4.65, N 5.65; found, C 87.19, H 4.68, N 5.61.

**Synthesis of Dendrimers.** The 1st-3rd generations of Dendrimers **G1**, **G2**, **G3** were synthesized in the similar procedure, so only a typical synthesis procedure for **G1** was described as follows: G<sub>1</sub>-B(OH)<sub>2</sub> (0.35 g, 12 mmol), tris(4-bromophenyl)amine (0.1 g, 0.2 mmol), and tetrakis(triphenylphosphine) palladium (0.0233 g, 0.02 mmol) were added to an air-free two-phase system composed of toluene (30 mL) and 2 M K<sub>2</sub>CO<sub>3</sub> aqueous solution (10 mL). The resultant mixture was vigorously stirred under an argon atmosphere at 80 °C for 24 h. The organic layer was separated and the aqueous phase was extracted with diethyl ether three times. The organic layers were combined and washed with brine and dried over anhydrous MgSO<sub>4</sub>. The solvent was evaporated and the residue went through silica-gel column.

**G1:** Yield 85% (0.12 g, 0.124 mmol); m.p. >300 °C; <sup>1</sup>H NMR (400 MHz, CDCl<sub>3</sub>):  $\delta$  = 8.17 (d, <sup>3</sup>J(H,H) = 7.6 Hz, 6H; Ar-H), 7.84 (d, <sup>3</sup>J(H,H) = 8 Hz, 6H; Ar-H), 7.68-7.64 (m, 12H; Ar-H), 7.49 (d, <sup>3</sup>J(H,H) = 8 Hz, 6H; Ar-H), 7.43 (t, <sup>3</sup>J(H,H) = 6.8 Hz, 6H; Ar-H), 7.36 (d, <sup>3</sup>J(H,H) = 7.6 Hz, 6H; Ar-H), 7.31 ppm (t, <sup>3</sup>J(H,H) = 7.6 Hz, 6H; Ar-H); IR (KBr):  $\tilde{\nu}$  = 3042 (C-H), 1598 (C=C), 1500 (C=C), 1451 (C=C), 1333 (C-N), 1066, 814 (C-H), 748 (C-H) cm<sup>-1</sup>; <sup>13</sup>C NMR (CDCl<sub>3</sub>, 100MHz):  $\delta$  = 147.1, 140.7, 139.7, 136.5, 134.8, 127.9, 127.4, 126.0, 124.6, 123.4, 120.4, 120.0, 109.8 ppm; MS (MALDI-TOF): *m/z* calcd for C<sub>72</sub>H<sub>48</sub>N<sub>4</sub>: 969.18; found: 968.40; elemental analysis calcd (%) for C<sub>72</sub>H<sub>48</sub>N<sub>4</sub>: C 89.23, H 4.99, N 5.78; found: C 89.20, H 4.96, N 5.82.

**G2:** Yield 72% (0.09 g, 0.037 mmol); m.p. >300 °C; <sup>1</sup>H NMR (400 MHz, CDCl<sub>3</sub>):  $\delta$  = 8.59 (s, 6H; Ar-H), 8.19 (d, <sup>3</sup>J(H,H) = 7.6 Hz, 12H; Ar-H), 8.00 (d, <sup>3</sup>J(H,H) = 6.8 Hz, 12H; Ar-H), 7.95 (d, <sup>3</sup>J(H,H) = 7.6 Hz, 6H; Ar-H), 7.85 (d, <sup>3</sup>J(H,H) = 7.6 Hz, 6H; Ar-H), 7.80-7.76 (m, 30H; Ar-H), 7.53 (d, <sup>3</sup>J(H,H) = 7.6 Hz, 12H; Ar-H), 7.46 (m, 18H; Ar-H), 7.32 ppm (t, <sup>3</sup>J(H,H) = 6.8 Hz, 12H; Ar-H); IR (KBr):  $\tilde{\nu}$  = 3044 (C-H), 1600 (C=C), 1500 (C=C), 1453 (C=C), 1335 (C-N), 1069, 817 (C-H), 751 (C-H) cm<sup>-1</sup>; <sup>13</sup>C

[View Online](#)

NMR (CDCl<sub>3</sub>, 100MHz):  $\delta$  = 147.0, 141.1, 141.0, 139.6, 136.3, 134.9, 132.8, 128.6, 127.4, 125.9, 124.7, 124.1, 123.4, 120.4, 120.0, 119.2, 110.8, 109.8 ppm; MS (MALDI-TOF):  $m/z$  calcd for C<sub>180</sub>H<sub>114</sub>N<sub>10</sub>: 2416.93; found 2423.48; elemental analysis calcd (%) for C<sub>180</sub>H<sub>114</sub>N<sub>10</sub>: C 89.45, H 4.75, N 5.80; found: C 89.49, H 4.71, N 5.75.

**G3**: Yield 43% (0.054 g, 0.01 mmol); m.p. >300 °C; <sup>1</sup>H NMR (400 MHz, CDCl<sub>3</sub>):  $\delta$  = 8.64 (s, 6H; Ar-H), 8.58 (s, 12H; Ar-H), 8.17 (d, <sup>3</sup>J(H,H) = 7.6 Hz, 24H; Ar-H), 8.07 (d, <sup>3</sup>J(H,H) = 7.2 Hz, 12H; Ar-H), 7.99 (d, <sup>3</sup>J(H,H) = 7.6 Hz, 24H; Ar-H), 7.93-7.75 (m, 48H; Ar-H), 7.70-7.67 (m, 42H; Ar-H), 7.52 (d, <sup>3</sup>J(H,H) = 7.6 Hz, 24H; Ar-H), 7.45-7.38 (m, 30H; Ar-H), 7.30 ppm (t, <sup>3</sup>J(H,H) = 7.2 Hz, 24H; Ar-H); IR (KBr):  $\tilde{\nu}$  = 3046 (C-H), 1602 (C=C), 1503 (C=C), 1457 (C=C), 1338 (C-N), 1069, 818 (C-H), 751 (C-H) cm<sup>-1</sup>; <sup>13</sup>C NMR (CDCl<sub>3</sub>, 100MHz):  $\delta$  = 141.4, 141.1, 136.4, 133.2, 128.8, 127.5, 126.1, 124.4, 123.5, 120.6, 120.2, 119.3, 110.9, 110.1 ppm; MS (MALDI-TOF):  $m/z$  calcd for C<sub>396</sub>H<sub>246</sub>N<sub>22</sub>: 5312.34; found: 5334.95 [M + Na]<sup>+</sup>; elemental analysis calcd (%) for C<sub>396</sub>H<sub>246</sub>N<sub>22</sub>: C 89.53, H 4.67, N 5.80; found: C 89.57, H 4.65, N 5.77.

## References

- (a) O. A. Matthews, A. N. Shipway and J. F. Stoddart, *Prog. Polym. Sci.*, 1998, **23**, 1–56; (b) S. M. Grayson and J. M. Frechet, *Chem. Rev.*, 2001, **101**, 3819–3868.
- (a) A. K. Patri, J. F. Kukowska-Latallo and J. R. Baker, *Adv. Drug Delivery Rev.*, 2005, **57**, 2203–2214; (b) R. Esfand and D. A. Tomalia, *Drug Discovery Today*, 2001, **6**, 427–436; (c) F. M. H. de Groot, C. Albrecht, R. Koekkoek, P. H. Beusker and H. W. Scheeren, *Angew. Chem. Int. Ed.*, 2003, **42**, 4490–4494; (d) R. J. Amir, N. Pessah, M. Shamis and D. Shabat, *Angew. Chem. Int. Ed.*, 2003, **42**, 4494–4499.
- (a) S. D. Konda, M. Aref, S. Wang, M. Brechbiel and E. C. Wiener, *Bio. And Med.*, 2001, **12**, 104–113; (b) D. A. Fulton, E. M. Elemento, S. Aime, L. Chaabane and M. Botta, D. Parker, *Chem. Commun.*, 2006, 1064–1066; (c) J. L. Mynar, T. J. Lowery, D. E. Wemmer, A. Pines and J. M.

- Frechet, *J. Am. Chem. Soc.*, 2006, **128**, 6334–6335.
- 4 (a) G. Koten and J. T. B. H. Jastrzebski, *J. Mol. Catal. A: Chem.*, 1999, **146**, 317–323; (b) V. Maraval, R. Laurent, A. M. Caminade and J. P. Majoral, *Organometallics*, 2000, **19**, 4025–4029; (c) N. N. Hoover, B. J. Auten and B. D. Chandler, *J. Phys. Chem. B*, 2006, **110**, 8606–8612.
- 5 (a) B. Lohse, R. Vestberg, M. T. Ivanov, Soren Hvilsted, R. H. Berg, C. J. Hawker and P. S. Ramanujam, *Chem. Mater.*, 2006, **18**, 6715–6720; (b) T. H. Ghaddar, J. F. Wishart, D. W. Thompson, J. K. Whitesell and M. A. Fox, *J. Am. Chem. Soc.*, 2002, **124**, 8285–8289.
- 6 (a) J. P. Lu, P. F. Xia, P. K. Lo, Y. Tao and M. S. Wong, *Chem. Mater.*, 2006, **18**, 6194–6203; (b) N. Satoh, T. Nskashima and K. Yamamoto, *J. Am. Chem. Soc.*, 2005, **127**, 13030–13038; (c) T. Hasobe, Y. Kashiwagi, M. A. Absalom, J. Sly, K. Hosomizu, M. J. Crossley, H. Imahori, P. V. Kamat and S. Fukuzumi, *Adv. Mater.*, 2004, **16**, 975–979; (d) W. L. Rance, B. L. Rupert, W. J. Mitchell, M. E. Kose, D. S. Ginley, S. E. Shaheen, G. Rumbles and N. Kopidakis, *J. Phys. Chem. C*, 2010, **114**, 22269–22276.
- 7 (a) T. S. Qin, G. Zhou, H. Scheiber, R. E. Bauer, M. Baumgarten, C. E. Anson, E. J. W. List and K. Mullen, *Angew. Chem. Int. Ed.*, 2008, **47**, 8292–8296; (b) L. Zhao, C. Li, Y. Zhang, X. H. Zhu, J. B. Peng and Y. Cao, *Macromol. Rapid Commun.*, 2006, **27**, 914–920; (c) H. J. Zhang, X. J. Xu, W. F. Qiu, T. Qi, X. K. Gao, Y. Liu, K. Lu, C. Y. Du, G. Yu and Y. Q. Liu, *J. Phys. Chem. C*, 2008, **112**, 13258–13263; (d) J. You, G. Y. Li, R. J. Wang, Q. P. Nie, Z. G. Wang and J. Y. Li, *Phys. Chem. Chem. Phys.*, 2011, **13**, 17825–17830.
- 8 (a) Y. Hang, Z. P. Fei, M. H. Sun, Z. S. Bo and W. Z. Liang, *Macromol. Rapid Commun.*, 2007, **28**, 1017–1023; (b) P. Furuta, J. Brookes, M. E. Thompson and J. M. J. Frechet, *J. Am. Chem. Soc.*, 2003, **125**, 13165–13172; (c) M. Halim, J. N. G. Pillow, I. D. W. Samuel and P. L. Burn, *Adv. Mater.*, 1999, **11**, 371–374; (d) A. Herrmann, T. Weil, V. Sinigersky, U. M. Wiesler, T. Vosch, J. Hofkens and F. C. D. Schryver, K. Mullen, *Chem. Eur. J.*, 2001, **7**, 4844–4853.
- 9 (a) P. Du, W. H. Zhu, Y. Q. Xie, F. Zhao, C. F. Ku, Y. Cao, C. P. Chang and H. Tian,

[View Online](#)

- Macromolecules*, 2004, **37**, 4387–4398; (b) D. J. Liu, S. D. Feyter, M. Cotlet, A. Stefan, U. M. Wiesler, A. Herrmann, D. Grebel-Koehler, J. Q. Qu, K. Mullen and F. C. D. Schryver, *Macromolecules*, 2003, **36**, 5918–5925; (c) A. P. Kulkarni, C. J. Tonzola, A. Babel and S. A. Jenekhe, *Chem. Mater.*, 2004, **16**, 4556–4573; (d) J. M. Lupton, I. D. W. Samuel, R. Beavington, M. J. Frampton, P. L. Burn and H. Bassler, *Phys. Rev. B*, 2001, **63**, 155206.
- 10 K. Albrecht and K. Yamamoto, *J. Am. Chem. Soc.*, 2009, **131**, 2244–2251.
- 11 (a) R. M. Adhikari, R. Mondal, B. K. Shah and D. C. Neckers, *J. Org. Chem.*, 2007, **72**, 4727–4732; (b) K. L. Paik, N. S. Baek and H. K. Kim, *Macromolecules*, 2002, **35**, 6782–6791; (c) K. R. J. Thomas, J. T. Lin, Y. T. Tao and C. H. Chuen, *Chem. Mater.*, 2002, **14**, 3852–3859; (d) M. Sonntag and P. Stroehriegel, *Chem. Mater.*, 2004, **16**, 4736–4742.
- 12 (a) S. Tang, M. R. Liu, P. Lu, H. Xia, M. Li, Z. Q. Xie, F. Z. Shen, C. Gu, H. P. Wang, B. Yang and Y. G. Ma, *Adv. Funct. Mater.*, 2007, **17**, 2869–2877; (b) K. T. Wong, Y. H. Lin, H. H. Wu and F. Fungo, *Org. Lett.*, 2007, **9**, 4531–4534; (c) J. Yang, T. L. Ye, D. G. Ma and Q. Zhang, *Synth. Metal*, 2011, **161**, 330–334.
- 13 (a) Z. G. Zhu and J. S. Moore, *J. Org. Chem.*, 2000, **65**, 116–123; (b) Z. H. Li and M. S. Wong, *Org. Lett.* 2006, **8**, 1499–1502; (c) Y. Li, J. F. Ding, M. Day, Y. Tao, J. P. Lu and M. D'iorio, *Chem. Mater.*, 2004, **16**, 2165–2173; (d) V. Promarak, A. Punkvuang, T. Sudyoasuk, S. Jungsuttiwong, S. Saengsuwan, T. Keawin and K. Sirithip, *Tetrahedron*, 2007, **63**, 8881–8890.
- 14 (a) N. Satoh, J. S. Cho, M. Higuchi and K. Yamamoto, *J. Am. Chem. Soc.*, 2003, **125**, 8104–8106; (b) A. Kimoto, J. S. Cho, M. Higuchi and K. Yamamoto, *Macromolecules*, 2004, **37**, 5531–5537; (c) J. Natera, L. Otero, F. D'Eramo, L. Sereno and F. Fungo, *Macromolecules*, 2009, **42**, 626–635. (d) A. Hameurlaine and W. Dehaen, *Tetrahedron Lett.*, 2003, **44**, 957–959; (e) F. Loiseau, S. Campagna, A. Hameurlaine and W. Dehaen, *J. Am. Chem. Soc.*, 2005, **127**, 11352–11363; (f) K. Albrecht, Y. Kasai, A. Kimoto and K. Yamamoto, *Macromolecules*, 2004, **41**, 3793–3800; M. J. Xiong, Z. H. Li and S. Wong, *Aust. J. Chem.*, 2007, **60**, 603–607.

- 15 Z. H. Zhao, H. Jin, Y. X. Zhang, Z. H. Shen, D. C. Zou and X. H. Fan, *Macromolecules*, 2011, **44**, 1405–1413.
- 16 H. Q. Zhang, S. M. Wang, Y. Q. Li, B. Zhang, C. X. Du, X. J. Wan and Y. S. Chen, *Tetrahedron*, 2009, **65**, 4455–4463.
- 17 (a) G. S. Liou, Y. L. Yang, W. C. Chen and Y. O. Su, *J. Polym. Sci. Part A: Polym. Chem.*, 2007, **45**, 3292–3302; (b) H. W. Chang, K. H. Lin, C. C. Chueh, G. S. Liou and W. C. Chen, *J. Polym. Sci. Part A: Polym. Chem.*, 2009, **47**, 4037–4050.
- 18 (a) Z. Q. Gao, Z. H. Li, P. F. Xia, M. S. Wong, K. W. Cheah and C. H. Chen, *Adv. Funct. Mater.*, 2007, **17**, 3194–3199; (b) Z. Ge, T. Hayakawa, S. Ando, M. Ueda, T. Akiike, H. Miyamoto, T. Kajita and M. Kakimoto, *Chem. Mater.*, 2008, **20**, 2532–2537.
- 19 F. S. Liang, T. Kurata, H. Nishide and J. J. Kido, *J. Polym. Sci. Part A: Polym. Chem.*, 2005, **43**, 5765–5773.
- 20 Z. Zhao, J. H. Li, X. Chen, X. Wang, P. Lu and Y. Yang, *J. Org. Chem.*, 2009, **74**, 383–395.
- 21 Y. Lin, Z. K. Chen, T. L. Ye, Y. F. Dai, D. G. Ma, Z. Ma, Q. D. Liu and Y. Chen, *J. Polym. Sci. Part A: Polym. Chem.*, 2010, **48**, 292–301.
- 22 H. H. Sung and H. C. Lin, *Macromolecules*, 2004, **37**, 7945–7954.
- 23 Z. J. Ning, Z. Chen, Q. Zhang, Y. L. Yan, S. X. Qian, Y. Cao and H. Tian, *Adv. Funct. Mater.*, 2007, **17**, 3799–3807.
- 24 A. Kulasi, H. Yi and A. Iraqi, *J. Polym. Sci. Part A: Polym. Chem.*, 2007, **45**, 5957–5967.
- 25 J. P. Lu, P. F. Xia, P. K. Lo, Y. Tao and M. S. Wong, *Chem. Mater.*, 2006, **18**, 6194–6203.
- 26 A. Iraqi, T. G. Simmance, H. Yi, M. Stevenson and D. G. Lidzey, *Chem. Mater.*, 2006, **18**, 5789–5797.
- 27 Q. Peng, M. Li, S. Lu and X. Tang, *Macromol. Rapid Commun.*, 2007, **28**, 785–791.
- 28 F. I. Wu, P. I. Shih and C. F. Shu, *Macromolecules*, 2005, **38**, 9028–9036.
- 29 Q. Zhang, J. Chen, Y. Cheng, L. Wang, D. Ma, X. Jing and F. Wang, *J. Mater. Chem.*, 2004, **14**,

[View Online](#)

895–900.

- 30 A. L. Kanibolotsky, R. Berridge, P. J. Skabara, I. F. Perepichka, D. D. C. Bradley and M. Koeberg, *J. Am. Chem. Soc.*, 2004, **126**, 13695–13702.

## Graphic abstract

# Starburst dendrimers consisting of triphenylamine core and 9-phenylcarbazole-based dendrons: synthesis and property

Jia You, Guiyang Li and Zhonggang Wang\*

*State Key Laboratory of Fine Chemicals, Department of Polymer Science and Materials, School of*

*Chemical Engineering, Dalian University of Technology, Dalian 116023, P. R. China*

Email: zgwang@dlut.edu.cn

